Multi-Fluid Modeling of Magnetic Reconnection in Astrophysical and Laboratory Plasmas

Alejandro Alvarez Laguna

Aeronautics and Aerospace Department, von Karman Institute for Fluid Dynamics, Belgium, alejandro.alvarez.laguna@vki.ac.be

Supervisor: Herman Deconinck

Professor and Dean of the Faculty, Aeronautics and Aerospace Department, von Karman Institute for Fluid Dynamics, Belgium, deconinck@vki.ac.be

University Supervisor: Stefaan Poedts

Professor, KU Leuven, Centrum voor mathematische Plasma-Astrofysica, stefaan.poedts@wis.kuleuven.be

Abstract

Improved models for characterizing collisional and reactive magnetized partially ionized plasma are essential to understand the phenomena taking place in astrophysical and laboratory plasmas. Particularly, scenarios where dissipative processes and thermo-chemical inequilibrium play an important role are beyond the classical single-fluid MHD representation. The multi-fluid models that consider each particle species as a separate fluid offer an alternative approach especially suitable for those situations. In the present work, a multi-fluid model considering two fluids, neutrals and charged species, is applied to simulate the magnetic reconnection taking place in the chromosphere.

Keywords: Magnetohydrodynamics (MHD), Magnetic Fields, Plasmas, Magnetic Reconnection, Sun: Atmosphere.

1. Introduction

The activity of the Sun has a great impact in our technology and ultimately in today's modern society that strongly depends on communications and satellite operations. From a global socio-economic perspective, the most important manifestations of solar activity are the solar wind and solar eruptions, i.e. solar flares and coronal mass ejection (CMEs). The unsteady but continuous emission of particles at high speed and temperature from the Sun into the space can hinder human activity at different levels. Satellite operations can be seriously affected by plasma ejected during solar storms, producing important damages or the loss of some of them, like the Telstar 401 that was short cut in January 1997. More recently, in 2003, a solar storm caused disruptions in the airplane routes and the CME affected several communication satellites (two were total loss). Also, when the high energetic charged particles ejected from the Sun reach our atmosphere can produce the so-called Geo-magnetically Induced Currents (GICs) that cause hazards in oil pipelines and power grid outages. An example of the latter is the magnetic storm that burned a $36 million transformer in New Jersey and left 6 million people more than 10 hours without electrical power in Quebec in winter conditions (March 1989). As a matter of fact, the cost of a severe space storm has been estimated to be trillions of dollars for the first year after the storm with recovery times of 4 to 10 years (an order of magnitude more than that of Hurricane Katrina) [1].

It is therefore necessary to improve the understanding and modeling of the phenomena taking place in the Sun for enhancing the tools used for the space weather forecasting and eventually reducing its risk on our technology. Magnetic reconnection is a process especially significant in space weather since it has been long considered as a mechanism for creating transient phenomena in magnetized plasma. It oc-

curs when oppositely directed magnetic field lines in conducting plasma merge due to diffusive processes producing a change of topology. The rearrangement of magnetic field lines produces a change of the magnetic flux that due to the finite conductivity creates a current sheet. In addition, the reconnection process causes a conversion of magnetic energy into kinetic and thermal energy, heating up the flow and accelerating it up to very high speed in very small timescales.

There are a wide variety of astrophysical scenarios in which the magnetic reconnection plays an important role. It is considered to be a likely mechanism to heat the corona to a few million degrees, still one of the biggest mysteries in Heliophysics [2]. Also, in CMEs and solar flares it is considered as a triggering mechanism which is present during the onset and early stages of the ejection [3]. In the Earths magnetosphere it is said to produce the plasma outflow at the magnetotail that is driven by the Earths magnetic field into the atmosphere producing the aurorae borealis and the GICs [4].

In the present work, we will focus on studying the magnetic reconnection in the Sun chromosphere, following the work presented in [5]. Observational data [6] have unveiled that the magnetic reconnection is the driver mechanism for the chromospheric jets and the spicules. The former can have timescales of 200-1000 s and current sheet length scales up to 5 Mm, producing outflows of 10 km/s. On the other hand, the spicules are smaller but faster phenomena, that last 10-600 s in length scales up to 1 Mm causing outflows up to 20-150 km/s [5].

The main goal of this study is the validation, throughout the comparison with the literature [5], of the numerical methods designed and implemented. Therefore, it can be considered as the starting point of a research that will be extended during the PhD. Future works will be targeted towards the improvement of magnetic reconnection models using multi-fluid description able to overcome the limitations of the standard single-fluid MHD. The ultimate goal is the development of efficient numerical tools that will be able to integrate the magnetic reconnection models in full-scale domains representing coronal mass ejections with improved fidelity.

2. Modeling of the magnetic reconnection

Magnetic reconnection is a process that happens as a result of a diffusive mechanism that produces a decay in the electrical conductivity of the plasma. The frozen-in constrain that holds in ideal plasmas (with infinite conductivity) is broken in a small region of width δ and length L. In this region, the magnetic field lines reconnect producing a rate of magnetic flux that results in the formation of a current sheet. Thus, the non-dimensional magnetic reconnection rate is defined [7] as follows:

$$M = \frac{d\Phi/dt}{v_A B_i} \tag{1}$$

where Φ is the magnetic flux per unit length in the direction perpendicular to the plane containing the current sheet , v_A is the Alfven speed and B_i is the magnetic field evaluated upstream of the current sheet.

Therefore, it is obvious to realize that the classical ideal MHD equations that consider the conductivity to be infinite are not able to tackle the physics involved in the reconnection. Nevertheless, the resistive singlefluid theory has developed analytical models for 2D steady magnetic reconnection. The Sweet-Parker model [8] proposes a non-dimensional reconnection rate of the form:

$$M = R_m^{-1/2} \tag{2}$$

where

$$R_m = v_A L/\eta \tag{3}$$

is called the Lundquist number, and η is the resistivity.

However, the model is unable to explain the fast energy released by the solar flares or in chromospheric jets and spicules, providing reconnection rates several orders of magnitude smaller.

On the other hand, the Petschek model [9] predicts faster reconnections suggesting geometry different from the Sweet-Parker one, Eq. 4. However, the model assumes explicitly or tacitly that resistivity gives the configuration setup. Because of this controversial issue, the Petschek model has been gradually thrown back [10].

$$M = \frac{\pi}{8\ln(R_m)} \tag{4}$$

Therefore, it is necessary to consider alternative theories to model the reconnection. The multi-fluid models consider each particle species as a different fluid that interact among each other by means of collisions and chemical reactions, exchanging thus mass, momentum and energy in their interplay. Since the width of the diffusion region can be comparable to

the ion scales [4], therefore, the multi-fluid description are considered to capture diffusive effects that are completely neglected by the single-fluid theory.

In the literature, one can find several fluid closures accounting for the different behavior of the species of plasmas in presence of electromagnetic fields. Braginskii [11] derives a two-fluid formulation considering separate ions and electrons. In his seminal work, he proposes closures for the transport properties, accounting for the anisotropy introduced by the magnetic field. Similarly, Magin [12] proposes a multicomponent model separating heavy particles and electrons, treating the effect of the magnetic field on the transport properties. Most recently, Meier [13] has proposed a two-fluid model considering the charged particles and neutrals as separate fluids, considering both anisotropic effects in the plasma heat conduction due to the magnetic field and chemical reactions (ionization and recombination).

3. Governing Equations

The multi-fluid description used in the results shown hereafter is the model discussed in [13]. It is a two-fluid model that considers separately neutrals and charged species, i.e. hydrogen ions and electrons. The full set of equations considered comprises mass, momentum and total energy conservation for both fluids. The chemical reactions considered are electron impact ionization and radiative recombination. The excited states are not tracked, only an effective potential is assumed ϕ_{ion} for the ionization reaction. The plasma is assumed to be optically thin, so the radiation effects are completely lost from the system. Electrons are considered to be in thermal equilibrium with ions, allowing neutrals to be in non-LTE. Charge neutrality is assumed and the electrons inertia and viscosity is neglected. This simplifications yields the following system:

$$\frac{\partial \rho_i}{\partial t} + \nabla \cdot (\rho_i \vec{v}_i) = m_i(\Gamma_i^{ion} + \Gamma_i^{rec}), \tag{5}$$

$$\frac{\partial \rho_n}{\partial t} + \nabla \cdot (\rho_n \vec{v}_n) = m_n(\Gamma_n^{ion} + \Gamma_n^{rec}), \tag{6}$$

$$\frac{\partial \rho_i \vec{v}_i}{\partial t} + \nabla \cdot (\rho_i \vec{v}_i \vec{v}_i + p_i + p_e) = -\nabla \cdot (\pi_i) + \vec{j} \times \vec{B} + \vec{R}_i^{in} + \Gamma_i^{ion} m_i \vec{v}_n - \Gamma_n^{rec} m_i \vec{v}_i, \tag{7}$$

$$\frac{\partial \rho_n \vec{v}_n}{\partial t} + \nabla \cdot (\rho_n \vec{v}_n \vec{v}_n + p_n) = -\nabla \cdot (\pi_n) - \vec{R}_i^{in} - \Gamma_i^{ion} m_i \vec{v}_n + \Gamma_n^{rec} m_i \vec{v}_i, \tag{8}$$

$$\frac{\partial}{\partial t}\left(\varepsilon_i + \frac{p_e}{\gamma_e - 1}\right) + \nabla \cdot \left(\varepsilon_i \vec{v}_i + \frac{\gamma_e p_e}{\gamma_e - 1}\vec{v}_i + p_i \vec{v}_i\right) = -\nabla \cdot (\vec{v}_i \cdot \pi_i + \vec{q}_i + \vec{q}_e) + \vec{j} \cdot \vec{E} + \vec{v}_i \vec{R}_i^{in} + Q_i^{in} - \Gamma_n^{rec} \frac{1}{2} m_i v_i^2 - Q_n^{rec} + \Gamma_i^{ion}\left(\frac{1}{2} m_i v_n^2 - \phi_{ion}\right) + Q_i^{ion}, \tag{9}$$

$$\frac{\partial \varepsilon_n}{\partial t} + \nabla \cdot (\varepsilon_n \vec{v}_n + \vec{v}_n p_n) = -\nabla \cdot (\vec{v}_n \cdot \pi_n + \vec{q}_n) - \vec{v}_n \vec{R}_i^{in} + Q_n^{in} + \Gamma_n^{rec} \frac{1}{2} m_i v_i^2 + Q_n^{rec} - \Gamma_i^{ion} \frac{1}{2} m_i v_n^2 - Q_i^{ion} \tag{10}$$

Where the subindices i, e, n stand for ions, electrons and neutrals. The electrical current follows Ohm's law $\vec{E} + \vec{v}_i \times \vec{B} = \eta \vec{j}$ with the resistivity η assumed to be constant. The reaction rates Γ^{ion} and Γ^{rec} and the reaction energy production Q^{ion} and Q^{rec} are taken from [22] and [23]. The momentum and energy collisional terms $\vec{R}_\alpha^{\alpha\beta}$ and $Q_\alpha^{\alpha\beta}$ considered are discussed in [5]. Ions and neutrals viscosity stress tensor are assumed to be Newtonian, with constant viscosity. Neutrals heat conduction follows Fouriers law with constant thermal conductivity, whereas ions have anisotropic heat flux accounting for the effect of the magnetic field, described in [11]. The fluid are assumed to be perfect gases with $\gamma = 5/3$.

The electromagnetic influence is tackled with the Maxwell equations:

$$\frac{\partial \vec{B}}{\partial t} + \nabla \times \vec{E} = 0 \tag{11}$$

$$\frac{\partial \vec{E}}{\partial t} - c^2 \nabla \times \vec{B} = -\frac{\vec{j}}{\epsilon_0} \tag{12}$$

$$\nabla \cdot \vec{B} = 0 \tag{13}$$

$$\nabla \cdot \vec{E} = \frac{\rho_c}{\epsilon_0} \tag{14}$$

where ρ_c is the charge density that is assumed to be zero.

4. Numerical Modeling

4.1. Finite Volume Method

The results have been obtained using the FV solver for unstructured grids provided by the COOLFluiD platform [14]. The governing equations are written in conservative form, as follows:

$$\frac{d}{dt}\int_{\Omega_i}\mathbf{U}\,d\Omega+\oint_{\partial\Omega_i}\mathbf{F^c}\cdot\mathbf{n}\,d\Sigma=\oint_{\partial\Omega_i}\mathbf{F^d}\cdot\mathbf{n}\,d\Sigma+\int_{\Omega_i}\mathbf{S}\,d\Omega \tag{15}$$

The conservative form of Maxwell equations is found in [15]. The cell-centered FV discretization applies the integral conservation law to each cell, assuming the solution to be constant over the cell and storing the value at the centroid of it. In order to obtain second order accuracy in space, inverse-distance weighted least square reconstruction [16] is used. The multidimensional limiter of Venkatakhrisnan [17] is used to obtain oscillation free solutions. The discretization of the inviscid fluxes is explained hereafter.

4.2. Hyperbolic divergence cleaning for Maxwell equations

One of the biggest concerns in the development of a Maxwell solver is to satisfy the two divergence constrains Eq. 13 and Eq. 14 on the discrete level. The hyperbolic divergence cleaning method [19] is discussed to be an efficient way to enforce the constrains in Finite Volume solvers. Two lagrange multipliers ϕ and ψ are added in Maxwell equations as follows:

$$\frac{\partial\vec{B}}{\partial t}+\nabla\times\vec{E}+\gamma^2\nabla\Psi=0 \tag{16}$$

$$\frac{\partial\vec{E}}{\partial t}-c^2\nabla\times\vec{B}+\chi^2c^2\nabla\Phi=-\frac{\vec{j}}{\epsilon_0} \tag{17}$$

$$\frac{\partial\Psi}{\partial t}+c^2\nabla\cdot\vec{B}=0 \tag{18}$$

$$\frac{\partial\Phi}{\partial t}+\nabla\cdot\vec{E}=\frac{\rho_c}{\epsilon_0} \tag{19}$$

Artificial waves are introduced at speeds γc and χc that remove the errors in the fulfillment of the constrains. Therefore, the two scalar parameters γ and χ should be chosen to be ≥ 1.

4.3. Steger-warming scheme for Maxwell equations

The Steger-Warming scheme [18] splits the flux at the interface into positive and negative components based on the eigenvalue structure of the system as follows:

$$\mathbf{F^c}=\mathbf{A}_+\mathbf{U}^L+\mathbf{A}_-\mathbf{U}^R \tag{20}$$

where

$$\mathbf{A}=\frac{\partial\mathbf{F^c}}{\partial\mathbf{U}}=\mathbf{A}_-+\mathbf{A}_+\text{ and }\mathbf{A}_\pm=\mathbf{R}\Lambda_\pm\mathbf{R}^{-1} \tag{21}$$

where $\mathbf{R}$ is the matrix of right eigenvectors, $\Lambda_\pm$ the diagonal matrix of diagonal matrices with the positive and negative eigenvalues, $\mathbf{U}$ are the conservative variables. The discretization including the divergence cleaning method is discussed in [19]. The method is shown to work standalone and coupled with NS equations of a single conducting fluid [20].

4.4. AUSM scheme for fluid equations

AUSM-family schemes [21] split the inviscid flux of each fluid at the cell interface into the convective part and the pressure flux as follows:

$$\mathbf{F^c}=\mathbf{F^{conv}}+\mathbf{P} \tag{22}$$

with

$$\mathbf{F^{conv}}=\dot{m}\mathbf{\Psi}^{L/R} \tag{23}$$

$\dot{m}$ is the numerical mass flux at the interface and $\mathbf{\Psi}^{L/R}$ is a vector with the variables convected. The superindex L/R denotes that the values are taken from the left or the right neighboring cell to the cell interface as follows:

$$\mathbf{\Psi}=\begin{cases}(1,\ u,\ v,\ w,\ h)_L & \text{if } \dot{m}>0\\ (1,\ u,\ v,\ w,\ h)_R & \text{if } \dot{m}<0\end{cases} \tag{24}$$

The methods to compute the numerical mass flux $\dot{m}$ and the pressure $\mathbf{P}$ at the cell interface are discussed in [21] and [20].

4.5. Implicit time stepping

The resulting set of equations is a very stiff system since it has characteristic speeds ranging from the speed of light to the speed of sound of the different fluids. In order to deal with the strong time step requirements, implicit time stepping is used. The second-order accurate three-point Backward Euler is used:

$$\frac{3}{2}\mathbf{U}^{n+1}-2\mathbf{U}^n+\frac{1}{2}\mathbf{U}^{n-1}=\Delta t\,\mathbf{R}^{n+1} \tag{25}$$

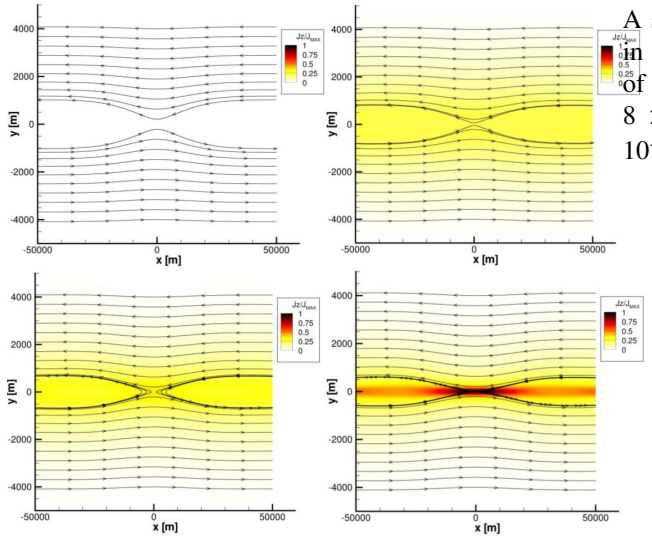

Figure 1: Evolution of the current sheet in the first seconds of simulation. Evolution of magnetic field lines and z-component of the electric current. Top: from left to right, $t = 0$ s and $t = 5$ s. Bottom: from left to right, $t = 10$ s and $t = 20$ s.

5. Results

The abovementioned model and numerical method are applied to reproduce a reconnection scenario under chromospheric conditions. The computational domain extends from -5×10^4 m to 5×10^4 m in the x direction and -5×10^3 m to -5×10^3 m in the y direction. Periodic boundary conditions are used in the x-direction and perfectly conducting boundaries in the y-direction. The simulation domain is divided into 182000 cells (1400×130). The mesh stretches in the center, where the reconnection takes place, up to sizes of the order of one meter, comparable to the neutral-ion collision mean free path.

The initial conditions are chosen to be similar to the middle chromospheric conditions estimated in the 1D model of the Sun [24]. The initial ion number density is $n_0 = 3.3 \times 10^{16} m^{-3}$ and the initial ionization level $n_i/(n_i + n_n) = 0.5\%$. The temperatures are set to 8750 K. A perturbation around the center in the temperature is imposed in order to create a pressure that balances the initial Lorentz force $T_i'(y) = 4366.49/\cosh^2(y/5000)$ K and $T_n'(y) = 5443.43/\cosh^2(y/5000)$ K. All the components of the velocity are set to zero excepting a small ions velocity in the vertical direction: $v_i(y) = 20.1 \tanh(y/5000)/\cosh^2(y/5000)$ m/s. The magnitude of the initial magnetic field is set to $1 \times 10^{-3} T$. A small perturbation around the center is introduced in order to obtain the reconnection in the center of the domain: $B_x = -1 \times 10^{-3} \tanh(y/5000) + 8 \times 10^{-9} y e^{-(x/20000)^2-(y/5000)^2}$ T and $B_y = -5 \times 10^{-10} x e^{-(x/20000)^2-(y/5000)^2}$ T.

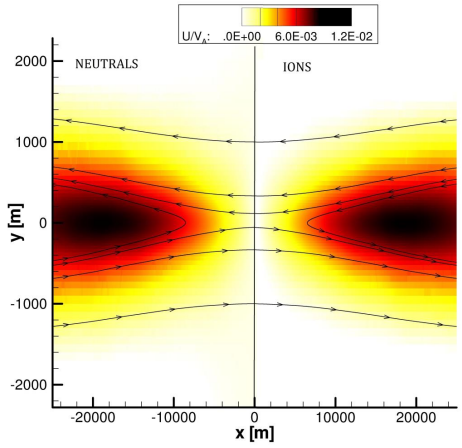

Figure 2: Horizontal velocity of neutrals and ions at $t = 20$ s. Non-dimensionalized with the value of the local Alfven speed outside the current sheet

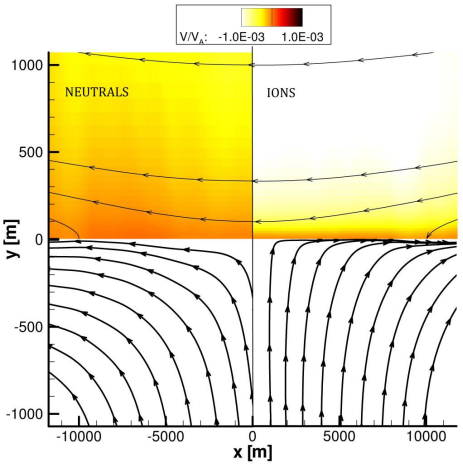

Figure 3: Vertical velocity and streamtraces of neutrals and ions at $t = 20$ s.

6. Conclusions

The first stages of a magnetic reconnection in the chromosphere have been simulated using a multi-fluid model considering two fluids, neutrals and charged particles. A current sheet is formed in the center of the domain, producing the acceleration of the ion fluid. The collisions drag the neutrals that have almost the same horizontal velocity, but much smaller vertical velocity. The results capture the phenomenology of the magnetic reconnection and agree with the literature. The numerical method, considering full set of Maxwell equations and using Finite Volume discretization is completely new. These results can be considered as the first steps that will be continued during the PhD targeted towards the study of the magnetic reconnection with multi-fluid models.

Acknowledgments

This research is funded through a fellowship provided by IWT (agentschap voor Innovatie door Wetenschap en Technologie). We would also like to thank Dr. Nagi N. Mansour for the supervision of this work at NASA Ames Research Center and Dr. Andrea Lani, COOLFluiD architect and advisor of this work.

References

[1] Committee on the Societal and Economic Impacts of Severe Space Weather Events, *Severe Space Weather Events Understanding Societal and Economic Impacts: A Workshop Report*, The National Academies Press, 2008.

[2] J. Birn and E. Priest, *Reconnection of Magnetic Fields*, Cambridge University Press, 2007.

[3] F. Zuccarello, *Data analysis and mathematical modeling of the initiation of coronal mass ejections*, PhD thesis, KU Leuven, 2012.

[4] M. Yamada, R. Kulsrud, and H. Ji, *Magnetic Reconnection*, Reviews of Modern Physics vol.82, 2010.

[5] J. E. Leake, V. Lukin, M. Linton and E. Meier, *Multi-fluid simulations of chromospheric magnetic reconnection*, ApJ. 760, 2012.

[6] K. Shibata et al., *Chromospheric Anemone Jets as Evidence of Ubiquitous Reconnection*, Science, Volume 318, Issue 5856, pp. 1591, 2008.

[7] K. Shibata and T. Magara, *Solar Flares: Magnetohydrodynamic Processes*, Living Rev. Solar Phys. 8, 2011.

[8] E. N. Parker, *Sweet's mechanism for merging magnetic fields in conducting fluids*, Geophysical research 62, No. 4, 509-520, 1957

[9] H. E. Petschek. *Magnetic Annihilation*. The Physics of Solar Flares, Proceedings of the AAS-NASA Symposium, October 1963

[10] D. Biskamp, *Magnetic Reconnection in Plasmas*, Cambridge University Press, 2005

[11] S. I. Braginskii, *Transport processes in a plasma*. Reviews of Plasma Physics, Volume 1., pp. 205 311. (1965)

[12] B. Graille , T. E. Magin , M. Massot, *Kinetic theory of plasmas. Translational Energy.* Mathematical Models and Methods in Applied Sciences, Vol. 19, 04 (2009) 527-599

[13] E. T. Meier, U. Shumlak, *A general nonlinear fluid model for reacting plasma-neutral mixtures.* Physics of Plasmas, Volume 19, Issue 7, pp. 072508-072508-11 (2012).

[14] A. Lani, *An object Oriented and high performmance platform for aerothermodynamics simulations*, PhD Thesis, von Karman Institute for Fluid Dynamics, 2009

[15] R. W. MacCormack. *Numerical Simulation of Aerodynamic Flow Including Induced Magnetic and Electric Fields.* In 39th AIAA Plasmadynamics and Lasers Conference, Seattle, June 2008.

[16] T. Barth. Aspects of unstructured grids and finite volume solvers for the euler and navier-stokes equations. 25th Computational Fluid Dynamics Lecture Series. Von Karman Institute, March 1994.

[17] V. Venkatakrishnan. *Convergence to steady state solutions of the euler equations on unstructured grids with limiters.* Journal of Computational Physics, 118:120130, 1995.

[18] J. Steger, R. F. Warming, *Flux vector splitting for the inviscid gas dynamic equations with application to finite difference methods*, J. Comp. Phys., Vol. 40, No. 2, pp. 263-293, 1981

[19] C.-D. Munz., P. Ommes, R. Schneider. *A three-dimensional finite-volume solver for the Maxwell equations with divergence cleaning on unstructured meshes*. Computer Physics Communications130, 83-117, December,1999.

[20] A. Alvarez, *Multi-Fluid MHD Development for Space Weather Modeling*, Research Master Report, von Karman Institute for Fluid Dynamics, June 2013.

[21] M. S. Liou, *A sequel to AUSM, part II: AUSM+ -up for all speeds.* J. Comp. Phys., 214:137170, 2006.

[22] G. S. Voronov, *A practical fit formula for ionization rate coefficients of atoms and ions by electron impact*, Atomic data nad nuclear data tables 65, 1-35, 1997

[23] B. M. Smirnov, *Physics of Atoms and Ions*, Springer-Verlag New York, Inc., 2003

[24] Vernazza, J. E., Avrett, E. H., Loeser, R., *Structure of the solar chromosphere. III. Models of the EUV brightness components of the quiet Sun*, ApJS45, 635-725, 1981